

SMART MIXERS AND REACTORS FOR THE PRODUCTION OF PHARMACEUTICAL NANOPARTICLES: PROOF OF CONCEPT

F. Lince*, D.L Marchisio and A.A. Barresi

*Dipartimento di Scienza dei Materiali ed Ingegneria Chimica, Politecnico di Torino,
Corso Duca degli Abruzzi 24, 10129, Torino, Italy;*

Abstract. In the pharmaceutical industry a growing number of applications employ polymeric nanoparticles. In order to produce suitable particulate systems it is important to accurately control both the particle size and morphology. In this work a methodology developed in our previous work is applied to the problem of turbulent precipitation by solvent displacement of poly- ϵ -caprolactone (PCL) and of poly-methoxypolyethyleneglycol-cyanoacrylate-co-hexadecyl cyanoacrylate P(MEPEGCA-co-HDCA) in water-acetone mixtures by using Confined Impinging Jets Reactors (CIJR). Our experimental data show that the effects of mixing and of the geometrical characteristics of the CIJR on the particle size distribution (PSD) are quite important, and the origin of these effects are interpreted by resorting to computational fluid dynamics (CFD) simulations. Eventually the possibility of exploiting these effects through an Adjustable Confined Impinging Jets Reactor (ACIJR) is demonstrated at a proof of concept level.

Key words: Nanoparticles; Solvent Displacement; CIJR; Poly- ϵ -caprolactone; P(MePEGCA-co-HDCA); Controlled Drug Delivery; Particle Size Distribution; Turbulent Mixing.

1. INTRODUCTION

In recent years colloidal particulate systems have attracted the interest of the scientific community owing to their interesting properties as drug carriers for therapeutic applications. Polymeric nanoparticles represent a very attractive system to achieve controlled drug release in order to prevent drug degradation and minimize toxic effects. However the final efficiency strongly depends on the physicochemical properties of the drug, such as its chemical structure, as well as on the structure of the carrier, and in particular its diameter and Particle Size Distribution (PSD) and surface properties. In fact, in order to avoid negative interactions with the Reticulo-Endotelial System (RES) particles must be smaller than 250 nm. Clearly, the efficiency of these systems may be strongly compromised by a short life time in the blood stream and a non-specific targeting [1,2].

Several methods exist to produce nanoparticles [3,4] and most of them involve mixing of two liquid streams and subsequent reaction steps. Particle formation is a complex process that includes several steps, namely particle nucleation, molecular growth and aggregation, and the rate of each of them determines the final PSD and other important properties. The driving force of these phenomena, both for reactive and non-reactive mixing, is the super-saturation. As it is well known, mixing plays a crucial role in the generation and redistribution of super-saturation which is connected to the nucleation and to the molecular growth rates.

In this work we focus on the solvent displacement technique [5] because it offers several important advantages, such as reproducible carrier sizes in the nanometric range, the use of ingredients with low toxic potential and also the possibility of controlling the PSD through mixing; the super-saturation in this case is defined as the ratio between the actual polymer concentration after mixing and the solubility of the polymer in the mixture of acetone and water, in the solvent mixture. Nucleation corresponds to the formation of new particles, called nuclei, whereas molecular growth is generally defined as the attachment of single polymer molecules onto the particle surface. A small increase in super-saturation can determine an increase of several orders of magnitude in the nucleation rate and only a small increase in the growth rate. As a consequence, at high super-saturation levels nucleation prevails over growth, and very small particles can be produced. The final PSD of the polymer particles is also affected by aggregation whose rate depends on the frequency of collision of polymer particles and on their stability. The entity of the repulsive forces can be estimated by measuring the zeta potential, which is the electrical potential near the particle surface and contains information on the stability of the colloidal system.

Solvent displacement applied to our system consists in a simple mixing operation that involves three main steps: dissolution of both polymer and drug into a solvent, mixing of the obtained solution with the anti-solvent, and eventually elimination of the solvent (usually through evaporation). Mixing leads to rapid diffusion of the solvent into the anti-solvent and spontaneous particle formation. However, since particle formation is extremely rapid, mixing must be very fast, and therefore special continuous mixers must be used; in this work Confined Impinging Jets Reactors (CIJR) are employed [6-9].

In this work particle formation by turbulent precipitation through solvent displacement of Poly- ϵ -caprolactone (PCL) and of Poly(methoxypolyethyleneglycol cyanoacrylate-co-hexadecyl cyanoacrylate) P(MEPEGCA-co-HDCA) nanoparticles is investigated. Acetone and water are used as solvent and anti-solvent, respectively. The aim of this work is to quantify the effect of mixing and of the reactor geometry on the final diameter. Our experimental data show that the main effect is related to the jets diameter, in fact, at a given flow rate (and therefore at a given residence time), a change in the jets diameter causes a change in the mixing dynamics and in the final diameter. The basic idea, demonstrated in this work at a proof of concept level, consists of a reactor with adjustable jets that can be manipulated in order to obtain particles within a specific size range for the requested applications.

2. EXPERIMENTAL SETUP AND OPERATING CONDITIONS

PCL with a molecular weight of $M_n = 80,000$ g/mol and P(MEPEGCA-co-HDCA) with a molecular weight approximately equal to 3,600 g/mol were used. Acetone (HPLC grade) and PCL were purchased from Sigma-Aldrich, whereas Millipore bi-distilled water was employed in all the experiments. P(MEPEGCA-co-HDCA) was synthesised directly by polycondensation of MePEGCA and HDCA with a 1 to 4 ratio. MePEGCA was obtained by esterification of cyanoacetic acid with metoxipolyethyleneglycole, while PHDCA was obtained by reaction between HDCA and formaldehyde in the presence of a catalyst. Details on the synthesis can be found in the original work of Peracchia and co-workers [11].

The molecular weights of the two polymers were determined through Dynamic Light Scattering (DLS) measurements (Zetasizer Nanoseries ZS, Malvern Instrument). In fact, according to the Debye theory, this information can be extracted by plotting the intensity of the scattered light of diluted samples of the polymer in a solvent at various concentrations and by comparing these measurements with that of the pure solvent. The scattered intensity was determined by averaging over several single measurements for the pure solvent (acetone) and

for the samples at various polymer concentrations. The obtained results were found to be in good agreement with the theoretical values.

In the CIJR the two solutions of solvent and anti-solvent are mixed in a very small volume in the centre of a cylindrical chamber, where due to collision and impingement of the two jets, turbulent kinetic energy is generated and then quickly dissipated; thanks to the geometry, bypass of the central region of intensive mixing is avoided. This reactor induces a very intense turbulent flow that leads to high mixing efficiencies, which allows production of very small particles. Characteristic mixing times have been estimated by Computational Fluid Dynamics (CFD) [9,10] and found to be of the order of millisecond.

As previously discussed the present study focuses on the development of a CIJR with adjustable diameter of the inlet jets. For this reason two different configurations, characterized by inlet jets diameter of 1 mm and 2 mm, are investigated. These two configurations will be indicated in the following as CIJR-d1 and CIJR-d2, respectively. The two investigated geometries are reported in Fig 1, and as it is possible to see they are identical but for the diameter of the inlet jets. For both geometries the two high velocity jets collide and mix in a small cylindrical chamber of 5 mm of internal diameter, and as already explained in our previous work the chamber head is conical as well as the outlet, with a fixed angle of 45°.

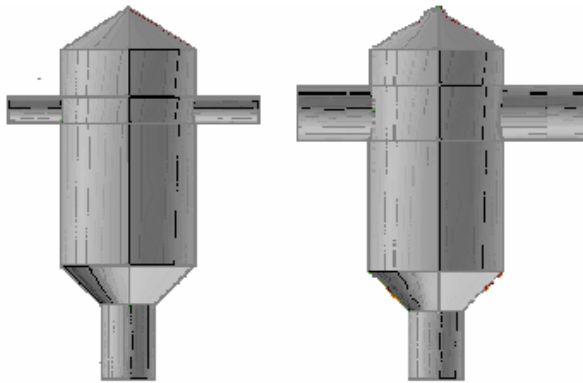


Figure 1. Sketches of the Confined Impinging Jets Reactor (CIJR) used in this work; on the left hand side CIJR-d1 ($d_j = 1$ mm) and on the right hand side CIJR-d2 ($d_j = 2$ mm).

The polymeric solution in acetone and the pure water solution were loaded in two syringes and fed into the reactors using a syringe pump (KDS200, KD Scientific). The outlet stream was quenched in a small volume of bi-distilled water, kept under gentle stirring and then sampled for PSD measurements through DLS. For the sake of brevity, although the PSDs were evaluated and analysed, in what follows only the final mean particle size (or diameter) will be reported.

Measurements were performed after precipitation by further dilution (1:2) with bi-distilled water.

Polymers were precipitated at constant temperature ($T = 30^\circ\text{C}$) under different operating conditions. The water and acetone flow rates (FR) were varied between 3 and 120 ml/min, while the final water to acetone ratio (W/A) was kept in between one and six.

Measurements were repeated three times in order to check the reproducibility of the synthesis and of the characterization protocol and results show an experimental uncertainty smaller than 8 % on mean particles size for PCL and of about 3% for P(MePEGCA-co-HDCA).

The operating conditions used for the different tests are summarized in Table 1, along with the Reynolds numbers (Re_j) in the inlet jets calculated for the acetone and water pure streams for the two reactor configurations.

The flow field and the mixing dynamics in the reactors were simulated by using FLUENT 6.3. whereas the computational grid was created with GAMBIT. Only half of the real geometry was considered, under the hypothesis of symmetry. Different grids were tested for both geometries and the final grid consisted of about 200,000 computational cells.

The fluid dynamics in the reactors is simulated by using averaged density and viscosity of the two fluids, as justified by some preliminary simulations carried out with variable properties of the pure fluids. Since the flow field in the inlet pipes is laminar, inlet velocity profiles were

defined by an elliptic paraboloid where the mean velocity is calculated on the basis of the flow rate for the two streams. Turbulence was modelled by using the Reynolds-Average Navier-Stokes approach (RANS) with the standard $k-\varepsilon$ model and with standard wall functions. A first-order upwind scheme was employed for spatial discretization, while for the pressure-velocity coupling the SIMPLE algorithm was employed.

Table 1. Operating conditions adopted for the precipitation tests

Operating parameter	Investigated values				
	<i>PCL</i>	<i>P(MePEGCA-co-HDCA)</i>			
Initial polymer concentration c_0 , mg/ml	<i>PCL</i>	1.5			
	<i>P(MePEGCA-co-HDCA)</i>	2			
Water to acetone flow rate ratio (W/A), -		1, 2, 3, 6			
Acetone flow rate (FR), ml/min	3	40	60	80	120
Water Jet Reynolds number $(Re_w)_{CIJR-d2}$, -	19	248	372	496	744
Water Jet Reynolds number $(Re_w)_{CIJR-d1}$, -	74	992	1488	1985	2977
Acetone Jet Reynolds number $(Re_A)_{CIJR-d2}$, -	40	535	802	1069	1604
Acetone Jet Reynolds number $(Re_A)_{CIJR-d1}$, -	160	2138	3207	4276	6414

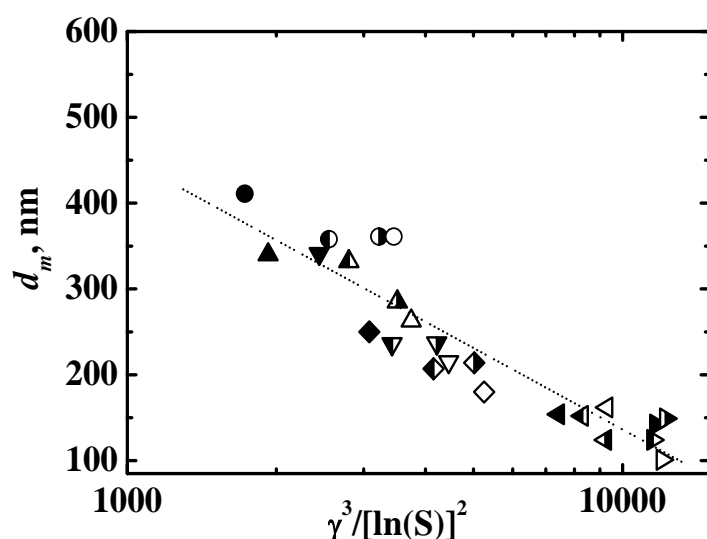


Figure 2. Mean particle size (d_m) of PCL versus the nucleation parameter $\gamma^3/[\ln(S)]^2$ for FR = 120 ml/min, $M_w = 80000$, obtained with the CIJR-d1 and with $c_0 = 4$ mg/ml (\circ), 3 mg/ml (\triangle), 1.5 mg/ml (∇), 1 mg/ml (\diamond), 0.2 mg/ml (\blacktriangleleft), 0.02 mg/ml (\blacktriangleright). Symbols filling W/A=1 filled, W/A=2 left-half filled, W/A=3 right-half filled and W/A=6 white.

Mixing dynamics was described by solving the transport equations for the mean mixture fraction and for the mixture fraction variance. The mixture fraction is a non-reacting scalar that lies between 0 and 1 and quantifies the level of segregation at the macro-scale in the reactor while the mixture fraction variance contains information concerning the level of segregation at the micro-scale [10].

The results presented in this work were obtained from simulations of flow field and mixing, by using a water to acetone ratio equal to one for the five different FRs indicated in Table 1. The solution of these additional transport equations was carried out with a user-defined subroutine.

Simulations were considered converged when the normalized residuals for each variable reached values smaller than 10^{-6} .

3. RESULTS AND DISCUSSION

According to the classical nucleation theory the nucleation rate at a fixed temperature is related to the interfacial tension γ between the nucleated particles and the solution (constituted by acetone and water) and the super-saturation ratio S . Our previous work suggests that the rate of polymer particle nucleation scales quite well with the classical nucleation parameter (i.e., $\gamma^3/[\ln(S)]^2$) that is used to correlate experiments carried out under different operating conditions, as plotted in Fig. 2. Details concerning γ and its measurements can be found in our previous work [12]. As it is seen from Fig. 2 experimental data points (obtained under almost instantaneous mixing conditions) scale quite well with this parameter, that can therefore be effectively used to define the operating conditions needed to produce particles with a specific final mean particle size.

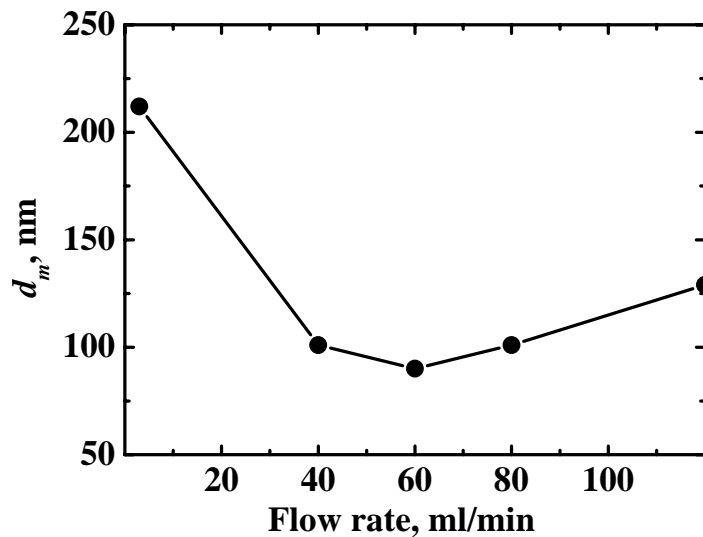


Figure 3. P(MePEGCA-co-HDCA) mean particle size (d_m) obtained with the CIJR-d1 versus the flow rate (FR) for $c_0 = 2$ mg/ml and water to acetone flow rate ratio $W/A=1$.

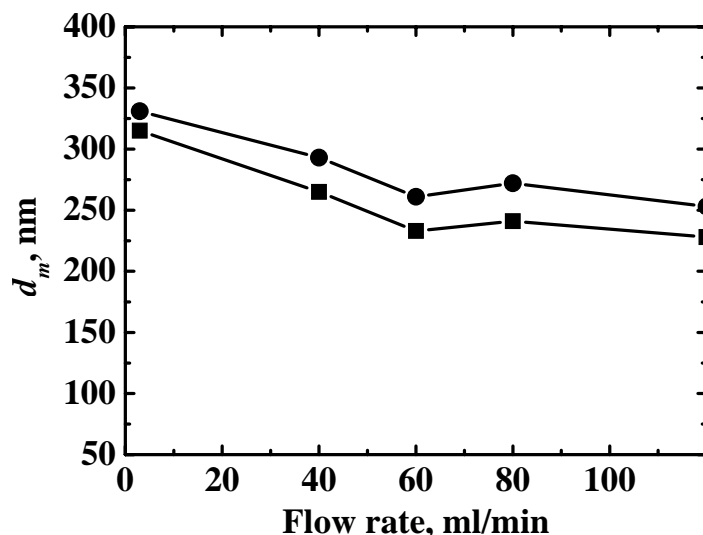


Figure 4. PCL mean particle size (d_m) versus the flow rate (FR) for $c_0 = 1.5$ mg/ml and water to acetone flow rate ratio $W/A=1$ obtained with the CIJR-d2 (●) and CIJR-d1 (■).

However these perfect mixing conditions are achieved only at the highest flow rates, whereas as the flow rate is reduced, and poor mixing conditions are achieved, the mean particle size can be significantly affected. The strong effect of the FR on the mean particle size is reported in Fig. 3. In this figure the P(MePEGCA-co-HDCA) mean particle size (d_m) is reported versus flow rate (FR), for the water to acetone ratio equal to one and for the small reactor.

As it is seen, increasing the flow rate of the solutions fed to the CIJR and thus improving mixing, nucleation is favoured over growth and the mean particle size is reduced. However, when the FR is increased beyond a critical value (i.e., $FR = 60$ ml/min), particle aggregation, induced by turbulent fluctuations, starts being important, resulting in a small increase of the mean particle size. In fact, as it is possible to notice, a minimum exists for a specific FR at about 40-60 ml/min.

In Fig. 4 the same results are reported for the two CIJR (i.e., CIJR-d1 and d2) for PCL and an initial polymer concentration equal to 1.5 mg/ml. As it is seen, the effect of mixing in both cases is relevant; moreover, it is also

possible to highlight that two regions exist: one at flow rate values smaller than 60 ml/min, where the effect on the mean particle size is relevant, and one for FR values greater than 60 ml/min, where an increase in FR does not affect much the final mean particle size. Analogous

trends were detected for the precipitation tests performed with different water to acetone ratios, especially for ratios equal to 6. This can be explained in terms of precipitation characteristic time-scales: when the FR rate is increased the characteristic mixing time is reduced, nucleation is favoured over growth and particles get smaller and smaller, but when the mixing time becomes smaller than the characteristic particle formation time-scale, no further reduction is detected (if aggregation is not relevant).

Further observation of Fig. 4 suggests that both the FR and the reactor geometry can affect the mean particle size and both must be taken into account for proper design and scale up. In fact, by increasing and decreasing the FR a significant variation in the mean particle size (i.e., from 350 to 200 nm) is observed, and by changing the jets diameter the same effect is obtained.

More information can be gathered by analyzing the results of the CFD simulations. In Fig. 5 the contour plots for the velocity magnitude for CIJR-d2 (left) and CIJR-d1 (right) are reported for a given FR. As it is possible to see, the two feed streams collide in the centre of the cylindrical chamber and determine an impinging plane where the turbulent kinetic energy is rapidly produced and then dissipated. For the CIJR-d2 the impinging plane is not well-defined when compared to CIJR-d1. This is caused by the different velocity of the fluid in the jets. For the CIJR-d1 the higher velocity of the fluid results in a more intense impingement of the jets and therefore in better mixing. This is confirmed by the contour plots of the turbulent intensity reported in Fig. 6. As it is seen, for a given flow rate (i.e., FR = 80 ml/min) the turbulent intensity reaches a maximum value of 23 % for the CIJR-d2, while for the same flow rate in CIJR-d1 a maximum value of 60 % is reached. As a consequence, a decrease in the jets diameter, for a constant flow rate, results in an increase of the jet velocity, that leads to a reduction of the thickness of the impinging plane, in higher values of the turbulence kinetic energy and in a significant improvement of the mixing efficiency. Because the flow rate remains constant, and because by changing the jets diameter the volume of the reactor remains constant too, the better mixing conditions are obtained by working under the same mean residence time (the contrary happens when the FR is changed).

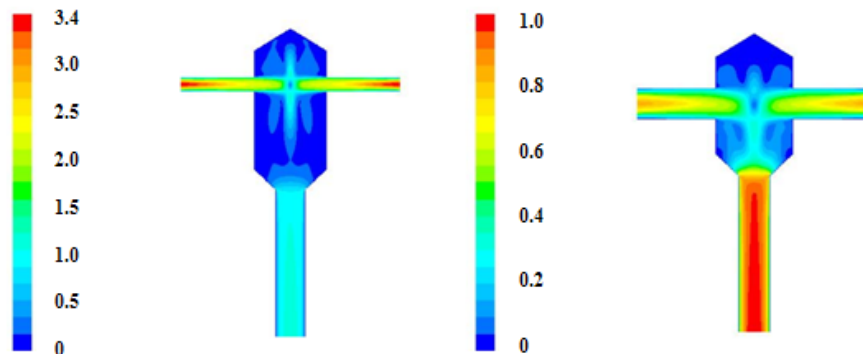


Figure 5. Contour plots for the velocity magnitude (m/s) at FR = 80 ml/min for CIJR-d1 (left) and CIJR-d2 (right).

This is confirmed by the contour plots of the mean mixture fraction for FR = 80 ml/min and for the CIJR-d2 and CIJR-d1 reported in Fig. 7. While for the CIJR-d1 the mean mixture fraction is almost everywhere equal to the complete mixing condition (i.e., 0.5) except for the two inlets, in the CIJR-d2 the perfect mixing condition is not reached everywhere, and still at the outlet some macro-scale gradients are detectable.

In Fig. 8 the contour plots of the mixture fraction variance is reported again for the CIJR-d2 and CIJR-d1. As it is seen, also for the level of segregation at the micro-scale, the effect of the geometry of the reactor is the same. For the CIJR-d2 the low jets velocity results in high mixture fraction variance values, and the micro-segregated region includes a quite large fraction of the volume of the reactor. For the CIJR-d1 instead the higher jets velocity results

in higher turbulence, higher mixture fraction variance dissipation rates and therefore smaller variance values. This smaller values imply smaller micro-scale segregation and therefore faster mixing. By comparing the left and right parts of Figs. 5, 6, 7 and 8, it is possible to conclude that mixing can be significantly improved by increasing the jets velocity at a constant flow rate by decreasing the jets diameter.

This improvement results then in a significant change of the mean particle size, as demonstrated in Fig. 4 and as shown by other experimental data not reported here for the sake of brevity. The different situations described above could be obtained in a single reactor with a constant chamber geometry and adjustable inlet jets, allowing to tune the mixing rate, by keeping a constant flow rate, and therefore with a constant mean residence time of the reactants in the reactor.

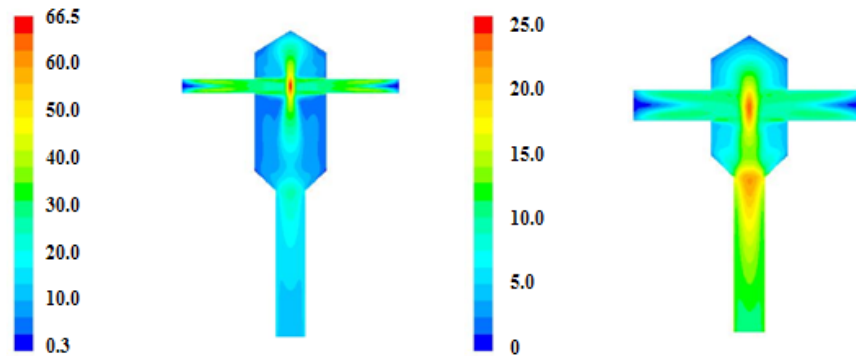


Figure 6. Contour plots for the turbulent intensity (%) at FR = 80 ml/min for CIJR-d1 (left) and CIJR-d2 (right).

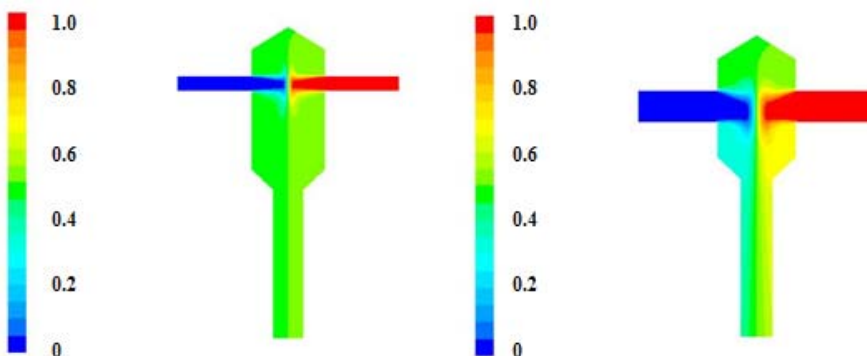


Figure 7. Contour plots for the mean mixture fraction at FR = 80 ml/min for CIJR-d1 (left) and CIJR-d2 (right).

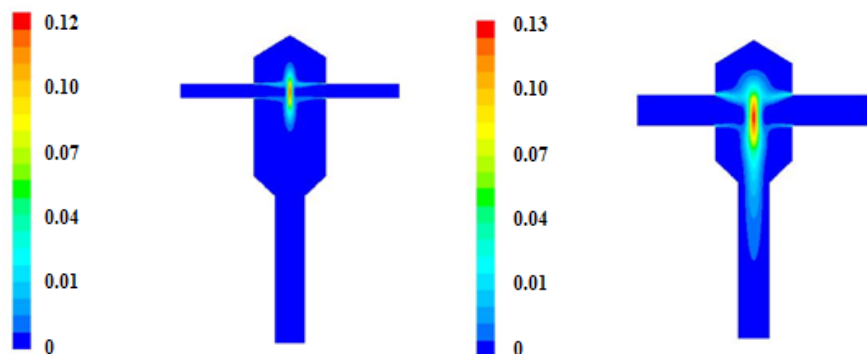


Figure 8. Contour plots for the mixture fraction variance at FR = 80 ml/min for CIJR-d1 (left) and CIJR-d2 (right).

3. CONCLUSIONS

In this work particle formation by turbulent precipitation through solvent displacement of Poly- ϵ -caprolactone (PCL) and Poly(methoxypolyethyleneglycol cyanoacrylate-co-hexadecyl

cyanoacrylate) P(MEPEGCA-co-HDCA) nanoparticles is investigated with different CIJR. Results show that the reactor geometry, notably the inlet jets diameter, affects the final mean particle size (and the underlying PSD) suggesting that a CIJR with adjustable inlet jets (i.e., Adjustable Confined Impinging Jets Reactor) could be more conveniently used to produce polymeric nanoparticles with specific characteristics. Our future work includes the assembling of a prototype and the assessment of the capabilities of the ACIJR by investigating the production of other particulate systems.

4. ACKNOWLEDGMENT

The authors gratefully acknowledge the contribution of Prof. Franco Dosio and Dr. Barbara Stella for the synthesis of P(MePEGCA-co-HDCA) and Giuseppe Casti for the precipitation experiments. The research has been partially supported by an Italian National Research Project (PRIN) "Multiscale Modelling and Development of Process Reactors for Polymeric Nanoparticle Precipitation".

5. REFERENCES

1. Stella B., Arpicco S., Pernacchia M.T., Desmaële D., Hoebeke J., Renoir M., d'Angelo J., Cattel L., Couvreur P., (2000), "Design of folic acid-conjugate nanoparticles for drug targeting", *J. Pharm. Sci.*, **89**, 1452-1464.
2. Petitti M., Barresi A.A., Vanni M., (2008), "Controlled release of vancomycin from PCL microparticles for an ophthalmic application", *Chem. Eng. Res. Des.*, submitted.
3. Soppimath K.S., Aminabhavi T.M., Kulkarni A.R., Rudzinski W.E., (2001), "Biodegradable polymeric nanoparticles as drug delivery devices", *J. Controlled Release*, **70**, 1-20.
4. Horn D., Rieger J., (2001), "Organic nanoparticles in aqueous phase", *Angew. Chem. Int. Ed.*, **40**, 4330-4361.
5. Fessi H., Puisieux F., Devissaguet J.P., (1989), "Nanocapsule formation by interfacial polymer deposition following solvent displacement", *Int. J. Pharm.*, **55**, R1-R4.
6. Johnson B.K., Prud'Homme R.K., (2003), "Chemical processing and micromixing in Confined Impinging Jets", *AIChE J.*, **49**, 2264-2282.
7. Johnson B.K., Prud'Homme R.K., (2003), "Flash nanoprecipitation of organic actives and block copolymers using Confined Impinging Jets Mixer", *Austral. J. Chem.*, **56**, 1021-1024.
8. Johnson B.K., Prud'Homme R.K., (2003), "Mechanism for rapid self-assembly of block copolymer nanoparticles", *Phys. Rev. Lett.*, **91**, 118302-1/4.
9. Marchisio D.L., Rivautella L., Barresi A.A., (2006), "Design and scale-up of chemical reactors for nano-particles precipitation", *AIChE J.*, **52**, 1877-1887.
10. Gavi E., Marchisio D.L., Barresi A.A., (2007), "CFD modelling and scale-up of Confined Impinging Jet Reactors", *Chem. Eng. Sci.*, **62**, 2228-2241.
11. Pernacchia M.T., Vauthier C., Desmaële D., Gulik A., Dedieu J.C., Demoy M., D'Angelo J., Couvreur P., (1998), "Pegylated nanoparticle from novel methoxypolyethylene glycol cyanoacrylate-hexadecyl cyanoacrylate amphiphilic copolymer", *Pharm. Research*, **15**, 550-556.
12. Lince F., Marchisio D.L., Barresi A.A., (2008), "Strategies to control the particle size distribution of poly- ϵ -caprolactone nanoparticles for pharmaceutical applications", *J. Colloid Interf. Sci.*, **322**, 505-515.